

## Level Structure of $\text{Ar}^{41}$ from the $\text{Ar}^{40}(d,p)\text{Ar}^{41}$ Reaction\*

E. KASHY, A. M. HOOGENBOOM,† AND W. W. BUECHNER

*Department of Physics and Laboratory for Nuclear Science, Massachusetts Institute of Technology, Cambridge, Massachusetts*

(Received August 7, 1961)

The energy-level structure of  $\text{Ar}^{41}$  has been investigated by bombarding argon gas with 7.5-Mev deuterons and measuring the energy spectrum and angular distributions of the reaction protons. A  $Q$  value of  $3.874 \pm 0.006$  Mev was measured. Fifty levels were observed, and their excitation energies,  $l_n$  values, reduced widths, and shell-model configurations have been determined. Mean energies of the shell-model configurations were:  $1f_{7/2}$ , 0 Mev;  $2p_{3/2}$ , 1.50 Mev;  $2p_{1/2}$ , 3.53 Mev;  $3s_{1/2}$ , 4.78 Mev;  $2d_{5/2}$ , 4.86 Mev; and  $1f_{5/2}$ , 5.55 Mev.

### I. INTRODUCTION

THE energy-level structure of  $\text{Ar}^{41}$  is of interest with regard to the shell model. The three  $f_{7/2}$  neutrons outside an almost closed proton shell give an energy-level scheme similar to that of  $\text{Ca}^{43}$  where the proton shell is closed.<sup>1</sup>

By measuring angular distributions and absolute values of differential cross sections for the  $\text{Ar}^{40}(d,p)\text{Ar}^{41}$  reaction, spins, parities, and reduced widths of levels in  $\text{Ar}^{41}$  have been determined. Previous work on this reaction<sup>2,3</sup> had given  $l_n$  values for 10 levels below 4 Mev. The present work is of higher resolution and was made possible by the development at the High Voltage Laboratory at M.I.T. of a thin-window rotating gas cell.<sup>4</sup>

### II. EXPERIMENTAL PROCEDURE

Deuterons were accelerated to 7.5 Mev by the MIT-ONR electrostatic accelerator and were deflected by a 90-deg analyzing magnet.<sup>5</sup> The exit slits of the analyzing magnet were adjusted to give a spread in incident energy of 0.14%. The incident beam, which averaged  $0.3 \mu\text{a}$ , entered a cylindrical rotating gas cell through a thin Formvar window. A diagram of the gas cell is shown in Fig. 1. Natural argon gas, which contains 99.6%  $\text{Ar}^{40}$  was used at a pressure of 0.81 cm of mercury as measured by the difference of levels in a calibrated oil manometer. The gas in the cell was continuously renewed by introducing it through a needle valve and allowing it to be removed through a second needle valve. The pressure was maintained constant by remote regulation of the second needle valve and monitoring of the manometer level using closed-circuit

television. The gas temperature was assumed to be the same as the cell temperature. The cell itself was maintained at constant temperature using cooling-water circulation.

The broad-range spectrograph, which has been described in detail elsewhere,<sup>6</sup> was provided with a set of vertical entrance slits close to the gas cell. The target thickness was defined by the width of these slits, the width of the incident deuteron beam, and the reaction angle. The target thickness was about 1.2 cm at 5 deg and was less than 0.6 cm for angles larger than 10 deg. This means that the energy loss in the target was less than 1.5 kev at all angles. The solid angle was defined by the width of the slit in the focal plane of the spectrograph, the length of the trajectory between this slit and the target, the angle of acceptance in the vertical direction, and the width of the vertical entrance slit of the spectrograph. The solid angle, which for a gas target is a function of angle, was calculated using a formula derived by Silverstein.<sup>7</sup> In addition, corrections were made to account for the effect of a beam stopper rotating with the gas cell. Considering the various errors of angle setting, we estimated the maximum error in mean angle of scattering at less than 1 deg.

An rms error of 6% in the final cross section was

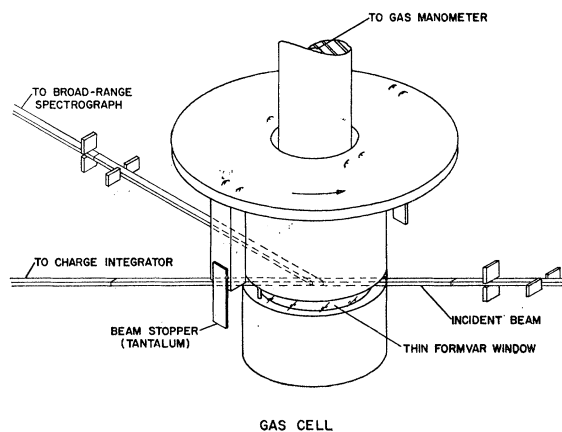


Fig. 1. Diagram of cylindrical gas cell showing the thin Formvar window and the tantalum beam stopper.

\* This work has been supported in part through an AEC contract with funds provided by the U. S. Atomic Energy Commission, by the Office of Naval Research, and by the Air Force Office of Scientific Research.

† Now at Instituut voor Kernfysisch Onderzoek, Amsterdam, The Netherlands.

<sup>1</sup> C. K. Bockelman, C. M. Braams, C. P. Browne, W. W. Buechner, R. D. Sharp, and A. Sperduto, *Phys. Rev.* **107**, 176 (1957).

<sup>2</sup> W. M. Gibson and E. E. Thomas, *Proc. Roy. Soc. (London)* **A210**, 543 (1952).

<sup>3</sup> H. B. Burrows, T. S. Green, S. Hinds, and R. Middleton, *Proc. Phys. Soc. (London)* **A69**, 310 (1956).

<sup>4</sup> A. M. Hoogenboom, *Rev. Sci. Instr.* (to be published).

<sup>5</sup> C. K. Bockelman, C. M. Braams, W. W. Buechner, and D. B. Guthe, *Phys. Rev.* **91**, 1502 (1953).

<sup>6</sup> C. P. Browne and W. W. Buechner, *Rev. Sci. Instr.* **27**, 899 (1956).

<sup>7</sup> E. A. Silverstein, *Nuclear Instr. and Methods* **4**, 53 (1959).

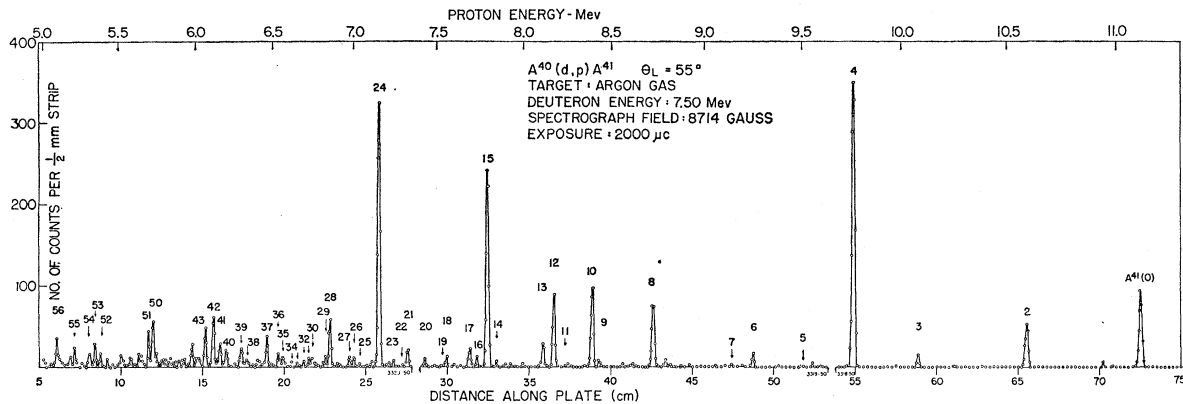


FIG. 2. Momentum spectrum of protons from the  $\text{Ar}^{40}(d,p)\text{Ar}^{41}$  reaction.

calculated from estimates of errors in pressure, temperature, solid angle, and charge integration. This error does not include any statistical error of counting. The nuclear emulsions were counted for proton tracks in half-millimeter strips across the exposed zone. During exposure, the emulsions had been covered with aluminum foils of sufficient thickness to stop the elastically and inelastically scattered deuterons from the target, but thin enough to allow the passage of the reaction protons. The elastically scattered deuterons, whose yield at 5 deg would have been large enough to produce sufficient  $\text{Al}^{27}(d,p)$  protons in the foil to obscure much of the plate, had a higher  $B\rho$  value than the  $\text{Ar}^{41}$  ground-state protons, and therefore caused no trouble.

The data for the various angles were obtained over a period of several weeks. There was not an internormalization of cross section, since each measurement resulted in an independent absolute measurement of cross section.

### III. RESULTS

The  $\text{Ar}^{40}(d,p)\text{Ar}^{41}$  cross section was measured in 5-deg intervals for angles from 5 to 30 deg and at angles of 40, 55, 70, 90, 110, and 130 deg. Although the entire plates were scanned, the analysis above an excitation energy of 5.1 Mev has been limited to the more intense proton groups. In this region, the distance between peaks and the intensities of most peaks are small. A typical momentum spectrum, the 55-deg data, is shown in Fig. 2. There was no trouble in peak identification, since almost all of the peaks were due to  $\text{Ar}^{40}$ . Natural argon is practically monoisotopic, and the contamination of the gas was negligible, as observed from the spectrum of elastically scattered deuterons.

A number of peaks were very small, including the new level at 0.171 Mev, whose average cross section was  $0.05 \pm 0.01$  mb/sr. The almost complete lack of background that has characterized most of the gas-target data taken so far was most helpful in identifying

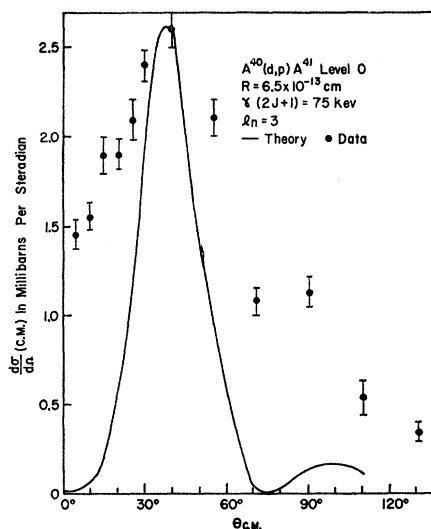


FIG. 3. Angular distribution of the protons to the  $\text{Ar}^{41}$  ground state.

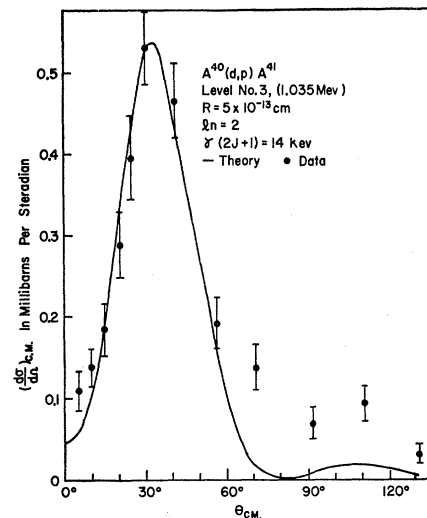


FIG. 4. Angular distribution of protons to the 1.035-Mev level in  $\text{Ar}^{41}$ .

TABLE I. Summary of the results for the energy-level scheme of Ar<sup>41</sup> and for the reduced widths of the levels.

Level	$E_x$ (Ar <sup>41</sup> ) (MeV)	$\theta_{\max}$ (deg)	$(d\sigma/d\Omega)_{\max}$		$l_n$	$\theta^2(2J+1)\times 10^{-3}$ $R=5.5f$	Shell-model configuration
			$\theta_{1/2}$ (deg)	mb/sr			
0	0.0	40	...	2.6	3	68	1f <sub>7/2</sub>
1	0.171±0.002	...	...	0.05	...	...	...
2	0.517±0.002	16	29	4.7	1	16	2p <sub>3/2</sub>
3	1.035±0.002	34	49	0.53	2	4.9	Core excitation
4	1.354±0.002	17	30	24.4	1	68	2p <sub>3/2</sub>
5	1.636±0.002	...	...	0.04	...	...	...
6	1.871±0.003	0	16	5.0	0	3.4	Core excitation
7	1.988±0.003	...	...	0.02	...	...	...
8	2.402±0.003	18	30	5.3	1	11.2	2p <sub>3/2</sub>
9	2.701±0.003	17	~25	0.67	1	1.3	2p <sub>3/2</sub>
10	2.740±0.004	16	28	5.8	1	11.3	2p <sub>3/2</sub>
11	2.895±0.004	0	18	0.57	0	0.4	...
12	2.955±0.004	18	31	4.1	1	7.5	2p <sub>1/2</sub>
13	3.017±0.004	18	29	1.9	1	3.4	2p <sub>1/2</sub>
14	3.293±0.005	15	27	0.49	1	0.83	2p <sub>1/2</sub>
15	3.335±0.005	15	29	11.1	1	18.8	2p <sub>1/2</sub>
16	3.393±0.005	~35	~60	0.14	3	2.9	...
17	3.438±0.005	~15	27	1.0	1	1.6	2p <sub>1/2</sub>
18	3.577±0.005	<sup>a</sup>	...	0.14	...	...	...
19	3.601±0.005	30	44	0.15	2	0.9	...
20	3.705±0.005	<sup>a</sup>	...	0.10	...	...	...
21	3.808±0.005	15	26	1.14	1	1.7	2p <sub>1/2</sub>
22	3.847±0.005	<sup>a</sup>	...	0.04	...	...	...
23	3.900±0.005	...	...	~0.02	...	...	...
24	3.979±0.005	15	28	12.4	1	17	2p <sub>1/2</sub>
25	4.108±0.006	...	...	~0.1	...	...	...
26	4.135±0.006	...	~28	0.2	...	...	...
27	4.163±0.006	...	46	0.18	(3)	...	...
28	4.280±0.006	13	28	2.4	1	3.0	2p <sub>1/2</sub>
29	4.305±0.006	0	18	0.48	(0)	...	...
30	4.395±0.006	0	22	1.18	...	...	...
31	4.414±0.006	...	...	0.10	...	...	...
				(40°)			
32	4.447±0.006	0	13	0.50	0	0.37	3s <sub>1/2</sub>
33	4.487±0.006	...	...	0.1	...	...	...
34	4.526±0.007	<sup>a</sup>	...	0.08	...	...	...
35	4.577±0.007	16	36	1.0	2	4.4	2d <sub>5/2</sub>
36	4.613±0.007	0	15	0.76	0	0.53	3s <sub>1/2</sub>
37	4.676±0.007	~20	37	1.7	2	7.24	2d <sub>5/2</sub>
38	4.816±0.008	<sup>a</sup>	...	0.09	...	...	...
39	4.840±0.008	18	54	0.52	3	8.7	1f <sub>5/2</sub>
40	4.935±0.008	0	16	1.9	0	1.3	3s <sub>1/2</sub>
41	4.977±0.008	...	40	0.8	...	...	...
42	5.018±0.008	10	28	2.5	1	3.3	...
43	5.070±0.008	~15	52	1.0	3	16	1f <sub>5/2</sub>
"50"	5.407±0.009	8	30	2.0	1	2.8	...
"51"	5.440±0.009	10	30	0.95	1	1.3	...
"52"	5.754±0.009	~10	~35	0.90	(2)	2.5	(2d <sub>5/2</sub> )
"53"	5.790±0.009	~10	36	0.75	2	1.8	2d <sub>5/2</sub>
"54"	5.825±0.009	...	~30	1.1	(1,2)	...	...
"55"	6.041±0.009	~20	52	0.7	3	9	1f <sub>5/2</sub>
"56"	6.146±0.009	~15	52	1.2	3	15	1f <sub>5/2</sub>

<sup>a</sup> Isotropic.

weak proton groups. In addition, the areas normally obscured by the C<sup>13</sup>(0) peaks were clear. The ground-state  $Q$  value was determined to be  $3.874\pm 0.006$  Mev by studying the reaction at a laboratory angle of 90 deg and using a stationary gas cell with small entrance and exit windows, both of which were made of Formvar. The exit window in that case was only of  $6\ \mu\text{g}/\text{cm}^2$  thickness, resulting in very small correction for energy losses. In all, 43 proton groups, corresponding to Ar<sup>41</sup> excited levels, were observed below 5.1 Mev, and an angular distribution was obtained for each. A list of the levels, their energy,  $E_x$ , angles of maximum cross

section  $\theta_{\max}$ , and their dimensionless reduced widths, calculated by using a radius of  $0.55\times 10^{-12}$  cm, is given in Table I. It was also found useful to tabulate the angle  $\theta_{1/2}$ , greater than  $\theta_{\max}$ , where the cross section had half its maximum value. This helped in the assignment of some of the higher levels, for which the angle of maximum cross section was not well defined.

In Figs. 3-6, we have plotted some of the angular distributions and their Butler-theory fits for  $l=3, 2, 1$ , and 0. All cross sections are given in the center-of-mass system, which only differs from the laboratory cross sections by a few percent because of the small velocity

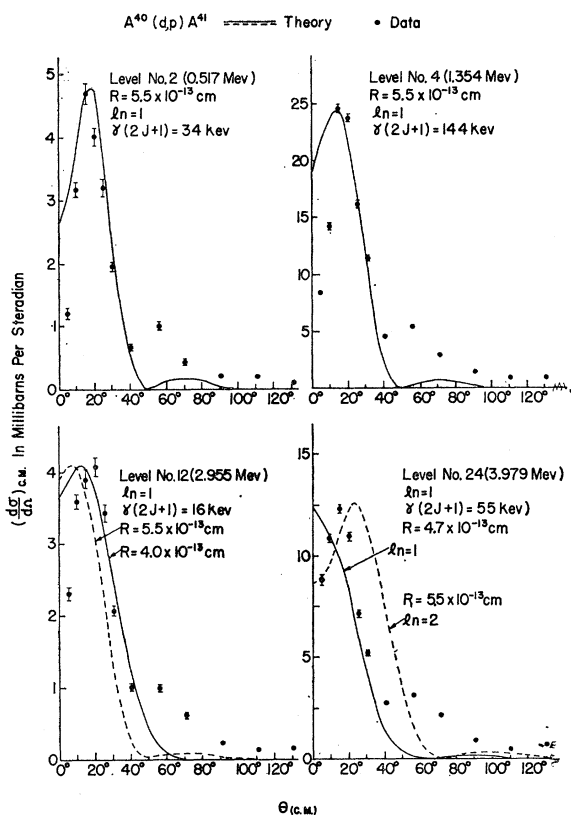


FIG. 5. Angular distribution of protons to levels in  $\text{Ar}^{41}$  at 0.517, 1.354, 2.955, and 3.979 Mev.

of the center of mass. Some of the proton groups did not exhibit a stripping pattern easily identified with a given  $l_n$  value. An example is peak (1), corresponding to the first excited level in  $\text{Ar}^{41}$ , whose angular distribution is given in Fig. 7.

#### IV. DISCUSSION

It is clear from the data in Figs. 3–6 that many of the angular distributions exhibit a strong forward-angle maximum characteristic of the stripping process. In order to compare the stripping theory to the experimental data, theoretical angular distributions were calculated using numerical tables of Enge and Graue,<sup>8</sup> which are based on formulas for stripping cross sections given by Friedman and Tobocman.<sup>9</sup> In order to obtain reduced widths for levels for which curves were not calculated, tables by Lubitz<sup>10</sup> giving numerical values of Butler stripping cross sections were also used. The review article written by Macfarlane and French<sup>11</sup>

<sup>8</sup> H. A. Enge and A. Graue, Univ. Bergen Arbok, Naturvitenskap, Rekke Nr. 13 (1955).

<sup>9</sup> F. L. Friedman and W. Tobocman, Phys. Rev. **92**, 93 (1953).

<sup>10</sup> C. R. Lubitz, "Numerical tables of Butler-Born approximation stripping cross sections," University of Michigan Report, 1957 (unpublished).

<sup>11</sup> M. H. Macfarlane and J. B. French, Revs. Modern Phys. **32**, 567 (1960).

which includes discussion of reduced widths from stripping reactions on nuclei in this part of the periodic table will also be used in the interpretation of our results.

A nuclear radius of 5.5 fermis was used in obtaining all reduced widths given in Table I. Once the  $l_n$  value for a given level was determined, the reduced width was calculated by matching the maximum of the theoretical differential cross section to the experimental cross section. This is not a very satisfactory way of obtaining the reduced width of levels, especially, in our case, for negative  $Q$  values. The theoretical curves do not give the correct position of maximum angle for reasonable values of the radius. Still, except in the  $l_n=0$  case, they give a reasonable estimate of the reduced width. For  $l_n=0$ , matching maximum cross sections does not work well at all. In Fig. 8,  $\theta^2(2J+1)/(\frac{d\sigma}{d\Omega})_{\text{max}}$  is plotted versus  $Q$  for  $l_n=0, 1, 2$ , and 3. Here  $\theta^2$  is the dimensionless reduced width,  $J$  is the spin of the  $\text{Ar}^{41}$  level, and  $(\frac{d\sigma}{d\Omega})_{\text{max}}$  is the maximum value of the differential cross section for protons to that level. As can be seen from the figure for  $l_n=0$ , that ratio becomes very large as  $Q$  becomes negative. The reason for the increase is that as  $Q$  becomes more negative, the theoretical stripping curves shift towards smaller angles much faster than the experimental stripping data. For example, the theoretical curves for  $l_n=0$  has shifted enough so that it has a minimum at  $\theta=0^\circ$  for  $Q=-2$  Mev. We can also see from Fig. 8 that the same effect appears for  $l_n=1$  around  $Q=-1$  Mev. This is clearly a weakness in the theory, since the experimental data show almost no shift toward smaller angles, while

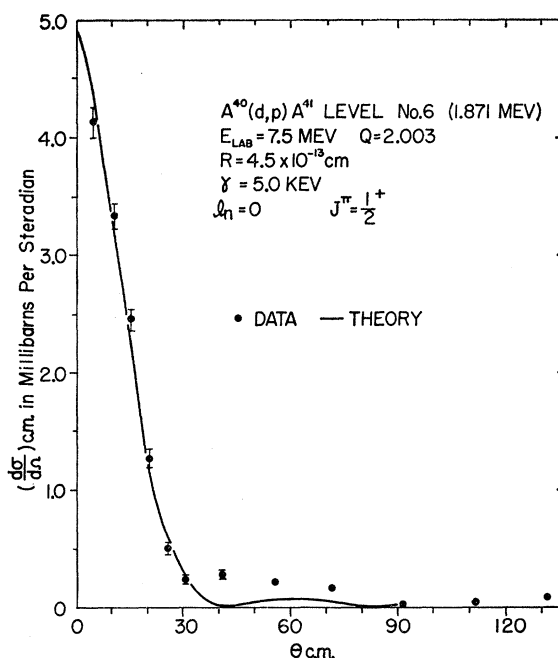


FIG. 6. Angular distribution of protons to the 1.871-Mev level in  $\text{Ar}^{41}$ .

the theoretical curves do. Figure 5 is a good illustration of this effect for four  $l_n=1$  levels. For excitation energies above 2 Mev, the dotted curve was used to obtain reduced widths for  $l_n=0$  levels.

In Figs. 3-6, the reduced width  $\gamma$  is given;  $\gamma$  has the dimension of energy and depends strongly upon the value chosen for  $R$ , the nuclear radius. This dependence decreases if the reduced width is expressed in terms of the Wigner limit,  $3\hbar^2/2\mu R^2$ . Thus, the dimensionless reduced width  $\theta^2 = \gamma(2\mu R^2/\hbar^2)$ . As an example, the ground-state angular distribution ( $J = \frac{7}{2}^-$ ) gave  $\gamma = 9.5$  and 18 kev for  $R = 6.5$  and 5.5 fermis, respectively. For  $\theta^2$ , the values are  $6.3 \times 10^{-3}$  and  $8.5 \times 10^{-3}$ . The values obtained for  $(2J+1)\theta^2$  are listed in Table I. These are also plotted in Fig. 9, together with the level scheme for Ar<sup>41</sup>. In the discussion that follows, not all levels of Table I are included. Those left out do not exhibit a clear stripping pattern and have very small cross sections.

### $l_n=3$ Transitions

The ground-state proton group was best fitted with  $l_n=3$  in agreement with the shell-model prediction that the Ar<sup>41</sup> ground state should be formed by the capture of a  $1f_{7/2}$  neutron in Ar<sup>40</sup>. The observed reduced width of  $\theta^2 = 0.0085$  is in agreement with  $\theta^2 = 0.01$ , as calculated by Macfarlane and French from previous data. As can be seen from Fig. 9, the next  $l_n=3$  transitions with reduced widths of importance consist of a group of four with a "mean energy"  $E_0 = (\sum E_i \theta_i^2 / \sum \theta_i^2)$  of 5.55 Mev. There is evidence that they belong to the  $1f_{5/2}$  configuration. From the independent-particle model, one would expect a single level for this configuration, corresponding to the eigenstate of the captured neutron in the potential of the target nucleus. The eigenstate is, in fact, not pure because of individual interactions between nucleons, thus resulting in many levels whose reduced widths are large for levels in the neighborhood

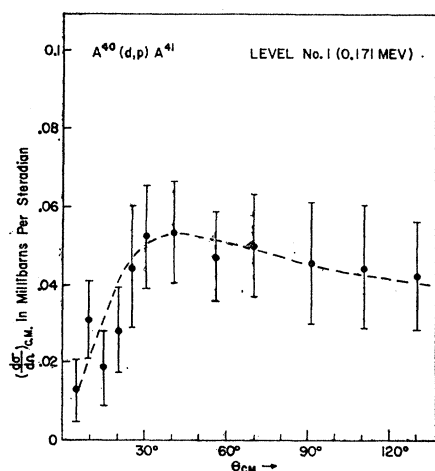


FIG. 7. Angular distribution of protons to the 0.171-Mev level in Ar<sup>41</sup>; the error bars represent the statistical error.

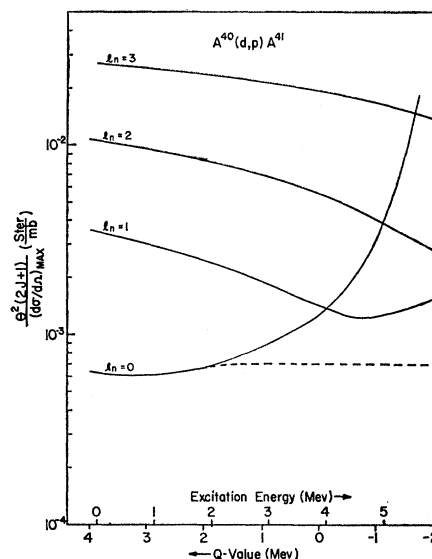


FIG. 8. Reduced widths corresponding to theoretical maxima of Butler curves versus excitation energies in Ar<sup>41</sup>.

of the pure eigenstate.<sup>12</sup> The high value of  $E_0$  for the  $1f_{5/2}$  configuration would explain why it has not been observed in the studies of  $(d,p)$  reactions for Ca isotopes. In addition, if these four levels, that is, levels Nos. 39, 43, "55", and "56", comprise nearly all the  $(1f_{5/2})$  fragments, we can apply the sum rule III.185 of reference 11:

$$\sum (2J+1)\theta^2 = \theta_0^2(2j+1)(2J_0+1),$$

where the summation on the left is over the fragments,  $j$  is the spin of the levels and, in this case, is  $\frac{5}{2}$ , and  $J_0$  is the spin of the target nucleus.  $\theta_0^2$  will be the  $1f_{5/2}$  single-particle reduced width. The result for  $\theta_0^2$ , using the values of  $(2J+1)\theta^2$  from Table I is  $\theta_0^2 = 0.0081$ , in excellent agreement with the  $1f_{7/2}$  value of 0.0085 for the pure ground state.

The previously unobserved low-lying level at 0.171 Mev is also of interest in discussing  $l_n=3$  transitions. There is little doubt that it corresponds to the 0.373 ( $\frac{5}{2}^-$ ) level in Ca<sup>43</sup> and to the 0.176-Mev level in Ca<sup>45</sup>. The angular distribution of the protons to the first level in Ar<sup>41</sup> does not suggest an  $l_n=3$  assignment, even though the cross section does go down at small angles. The cross section to this level (0.05 mb/sr) is small compared to 1 mb/sr for the level No. 43, the largest of the observed  $l_n=3$  levels around 5.5 Mev. If this level is assigned  $1f_{5/2}$ , one might understand its small cross section, since it would lie 5.3 Mev away from the main  $1f_{5/2}$  component.

### $l_n=2$ Transitions

All the  $l_n=2$  levels appear to be above 4.5 Mev, except for the  $l_n=2$  level at 1.035 Mev which was

<sup>12</sup> A. M. Lane, R. G. Thomas, and E. P. Wigner, Phys. Rev. 98, 693 (1955).

assigned  $J^\pi = \frac{3}{2}^+$  and a core-excitation origin,<sup>11</sup> and the weak level at 3.601 Mev. The other levels are assumed to belong to the  $2d_{5/2}$  configuration, with a mean energy  $E_0 = 4.86$  Mev. Calculating the single-particle  $2d_{5/2}$  reduced width with the assumption that those four levels (Nos. 35, 37, "52", and "53") comprise all of the main fragments, one obtains  $\theta_0^2 = 2.7 \times 10^{-3}$ . It is interesting to note that the four levels forming this group are split into two groups around 4.6 and 5.8 Mev. These seem to correspond to two  $l_n = 2$  levels observed in  $\text{Ca}^{40}(d,p)\text{Ca}^{41}$  by Holt and Marsham<sup>13</sup> at 4.76 and 5.72 Mev.

#### $l_n = 1$ Transitions

The  $l_n = 1$  levels not arising from core excitation should make up two sets of fragments of  $2p_{3/2}$  and  $2p_{1/2}$  shell-model states. In the initial separation into two groups, the levels 0.517 and 1.354 Mev were assigned  $2p_{3/2}$ , while all  $l_n = 1$  levels lying between 2.4 and 4.2 Mev were assumed to belong to the  $2p_{1/2}$  group. This division gave  $E_0(2p_{3/2}) = 1.20$  Mev and  $E_0(2p_{1/2}) = 3.23$  Mev, with the  $2p_{1/2} - 2p_{3/2}$  energy difference of 2.03 Mev almost identical to the 2.026-Mev separation found for  $\text{Ca}^{49}$  for the corresponding levels.<sup>14</sup> However, the calculated single-particle reduced widths yield  $\theta_0^2(2p_{3/2}) = 2.1 \times 10^{-2}$  and  $\theta_0^2(2p_{1/2}) = 3.9 \times 10^{-2}$ , and these are in poor agreement. In order to obtain better agreement,  $l_n = 1$  levels below 2.8 Mev were assigned to the  $2p_{3/2}$  configuration and those from 2.9 to 4.2 Mev were assigned to  $2p_{1/2}$  configuration. This division gave  $\theta_0^2(2p_{3/2}) = 2.7 \times 10^{-2}$  and also  $\theta_0^2(2p_{1/2}) = 2.7 \times 10^{-2}$ . The values for mean energies were  $E_0(2p_{3/2}) = 1.50$  Mev and  $E_0(2p_{1/2}) = 3.53$  Mev, with the difference of 2.03 Mev again in excellent agreement with the corresponding difference in  $\text{Ca}^{49}$ . The assignment of levels in one configuration or another cannot be certain, especially in this case where the levels are close together. There could easily be cross-overs. However, the mean energy would not change to any large extent.

#### $l_n = 0$ Transitions

Since  $\text{Ar}^{40}$  has spin  $0^+$ , all  $l_n = 0$  levels have  $J = \frac{1}{2}^+$ . The 1.871-Mev level is low lying and probably arises from core excitation. The three levels around 4.8 Mev, level Nos. 32, 36, and 40 have a mean energy  $E_0 = 4.78$  Mev, and, assuming they comprise the main  $3s_{1/2}$  fragments, have a single-particle reduced width  $\theta_0^2(3s_{1/2}) = 1.1 \times 10^{-3}$ .

<sup>13</sup> J. R. Holt and T. N. Marsham, Proc. Phys. Soc. (London) **A66**, 565 (1953).

<sup>14</sup> W. W. Buechner, *Proceedings of the 1954 Glasgow Conference on Nuclear and Meson Physics* (Pergamon Press, New York, 1954).

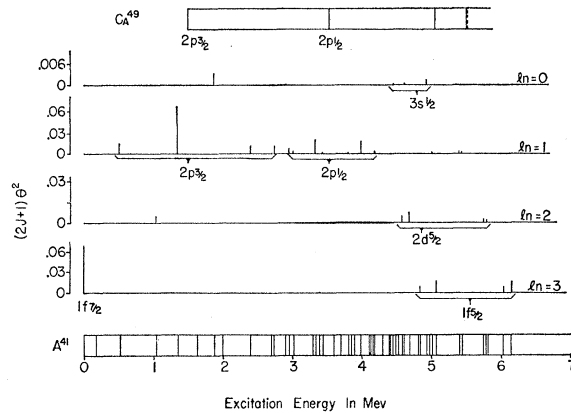


FIG. 9. Level scheme of  $\text{Ar}^{41}$  showing the reduced widths of the various levels.

The results obtained here for mean energies are in good agreement with previous work on other nuclei. The  $3s_{1/2} - 1f_{7/2}$  splitting of 4.78 Mev, the  $2d_{5/2} - 1f_{7/2}$  splitting of 4.86 Mev, and the  $2d_{5/2} - 2p_{1/2}$  splitting of 1.33 Mev agree well with work by Schiffer, Lee, and Zeidman<sup>15</sup> on  $\text{Ti}^{49}$  for which these values are 4.9, 4.3, and 1.2 Mev, respectively. The agreement of the  $2p_{1/2} - 2p_{3/2}$  energy difference with the results in  $\text{Ca}^{49}$  has already been discussed. The confirmation of the position of the  $1f_{5/2}$  single-particle configuration is shown in many ways. Levels in  $\text{Ca}^{49}$  have been observed at 2.026, 3.589, and 4.004 Mev, with the ground state and first-excited state constituting the  $2p_{3/2}$  and  $2p_{1/2}$  components, respectively. This indicates a  $1f_{5/2} - 2p_{3/2}$  spacing  $\geq 3.59$  Mev. In the  $\text{Ar}^{41}$  case, it is observed to be 4.05 Mev. Enge *et al.*,<sup>16</sup> in a study of  $\text{K}^{39}(d,p)\text{K}^{40}$  reaction, report a level at 6.06 Mev that possibly has  $l_n = 3$  and is associated with a  $d_{3/2} - 1f_{5/2}$  quadruplet. In their study of  $\text{Ca}^{40}(p,p)\text{Ca}^{40}$ , Class *et al.*,<sup>17</sup> find evidence for the main  $1f_{5/2}$  component in  $\text{Sc}^{41}$  at 5.8 Mev, in good agreement with the present result.

#### ACKNOWLEDGMENTS

Thanks are due to Mr. W. Tripp and to Mrs. Mary Fotis for their competent scanning of the nuclear emulsions. One of the authors (E.K.) wishes to thank the National Science Foundation for a fellowship he received from them that was in effect during the early part of this work.

<sup>15</sup> J. P. Schiffer, L. L. Lee, Jr., and B. Zeidman, Phys. Rev. **115**, 427 (1959).

<sup>16</sup> H. A. Enge, E. J. Irwin, Jr., and D. H. Weaner, Phys. Rev. **115**, 949 (1959).

<sup>17</sup> C. M. Class, R. H. Davis, and J. H. Johnson, Phys. Rev. Letters **3**, 41 (1959).